Electron Spin Resonance Imaging of Degradation and Stabilization Processes: Behavior of a Hindered Amine Stabilizer in UV-Exposed Poly(acrylonitrile−butadiene−styrene) Polymers

Mikhail V. Motyakin,[†] John L. Gerlock,[‡] and Shulamith Schlick*[,†]

Department of Chemistry, University of Detroit Mercy, Detroit, Michigan 48219-0900, and Mail Drop 3083/SRL, Ford Research Laboratory, Ford Motor Company, P.O. Box 2053, Dearborn, Michigan 48121-2053

Received March 23, 1999

Introduction. Polymeric materials exposed to heat, mechanical stress, and ionizing or UV irradiation undergo degradation in the presence of oxygen due to the formation of reactive intermediates such as free radicals R•, RO•, and ROO• and hydroperoxides ROOH.[1−10] The degradation process can be accelerated by chromophores, free radicals, and metallic residues from the polymerization reactions. The structural and morphological changes in the polymer properties due to exposure to environmental factors are often profound and include modification of the chemical structure (for instance, formation of double bonds, chain scission, and cross-linking) and loss of crystallinity, especially at large radiation doses. Often the deleterious effects are not immediately detected but develop over longer periods. The gradual changes in the polymer properties observed in many systems including polyolefins, and the ultimately grave results, are due to trapped radicals that react slowly, to peroxy radicals that decompose in time with formation of reactive radicals and gas molecules, and to trapped gases that lead to local stresses and to cracking.[3,9] While the time scale of these changes may vary, the final results are dramatic: degradation of the structure and collapse of the mechanical properties. The accelerated rate of ozone depletion in the stratosphere due to environmental factors is expected to raise the level of UV-B radiation ($\lambda = 290-320$ nm), thus adding severity to the problem of degradation and urgency to the need for solutions.

Hindered amine stabilizers (HAS) rank among the most important recent developments for light and heat stabilization of polymeric materials. Nitroxides and hydroxylamine ethers are the major products of reactions involving HAS. The HAS-derived nitroxides are thermally stable but can react with free radicals (as "scavengers") to yield diamagnetic species; the hydroxylamine ethers can regenerate the original nitroxide, thus resulting in an efficient protective effect.[6,9] The pivotal role of nitroxides (added as such or derived from HAS) has been documented recently in low-molecular-mass model systems.[7] In polymers the situation is more complicated, and the equilibrium concentration of the nitroxides varies markedly with the nature of the polymer matrix, thermal history, humidity, and type of HAS. At the present time, the complex protective mechanism offered by HAS is known only in broad terms.[6−11]

Chart 1

Repeating Units in ABS Polymers[19]

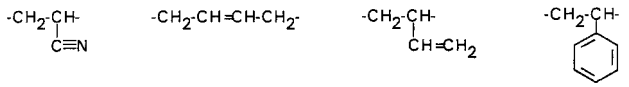

Hindered Amine Stabilizer (HAS): Tinuvin 770

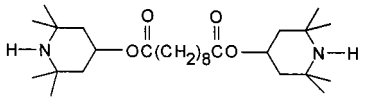

We present a study of HAS behavior in ABS polymers exposed to UV radiation using an imaging method derived from electron spin resonance spectroscopy: ESR imaging (ESRI). The technique is based on encoding spatial information in the ESR spectra via magnetic field gradients and provides information on the *spatial* distribution of paramagnetic species;[12] the direction of the field gradients determines the spatial directions that can be explored. Because ESR spectroscopy is a highly sensitive and specific method for the detection of species containing unpaired electron spins, imaging based on ESR is the method of choice for the detection of the *spatial* distribution of these species.

Experimental Section. *Sample Preparation.* The process of polymer degradation is gradual and slow. We have performed accelerated degradation experiments by exposure to UV irradiation of the polymer poly(acrylonitrile−butadiene−styrene) (ABS Magnum 342 EZ, from Dow Chemical Co.) doped with 2% w/w of (bis-(2,2,6,6-tetramethyl-4-piperidinyl) sebacate), a HAS known as Tinuvin 770 from Ciba Specialty Chemicals Corp. (Chart 1). The polymer and the HAS were blended at 100 rpm in a Boy Banbury mixer at 167 °C for 5 min, shredded, and shaped into 10 cm × 10 cm × 0.4 cm plaques in an injection molding machine at 210 °C. The plaques were exposed on one side to UV radiation in a Ci35 Weather-ometer equipped with borosilicate inner and outer filters and located at the Ford Research Laboratories. The chamber allows simultaneous control of the temperature (black panel temperature of 65 °C) and humidity (dew point 25 °C). The spectrum of the irradiation source in the chamber, from 295 nm into the IR region, mimics the range of the solar spectrum, and its intensity is continuously monitored by a sensor operating at 340 nm. The irradiation intensity, 0.45 W/m^2, is comparable with the average summer noontime solar intensity in Miami, FL.[13] The plaques were irradiated continuously. For the ESR imaging experiments we cut from the plaques cylindrical samples 4 mm long and ≈4 mm in diameter, with the cylinder axis along the direction of the UV radiation. The samples were placed in the ESR resonator with the symmetry axis along the field gradient and the irradiated part on top.

[†] University of Detroit Mercy.
[‡] Ford Research Laboratory, Ford Motor Company.
* Corresponding author. E-mail schlicks@udmercy.edu.

10.1021/ma9904363 CCC: $18.00
Published on Web 07/20/1999

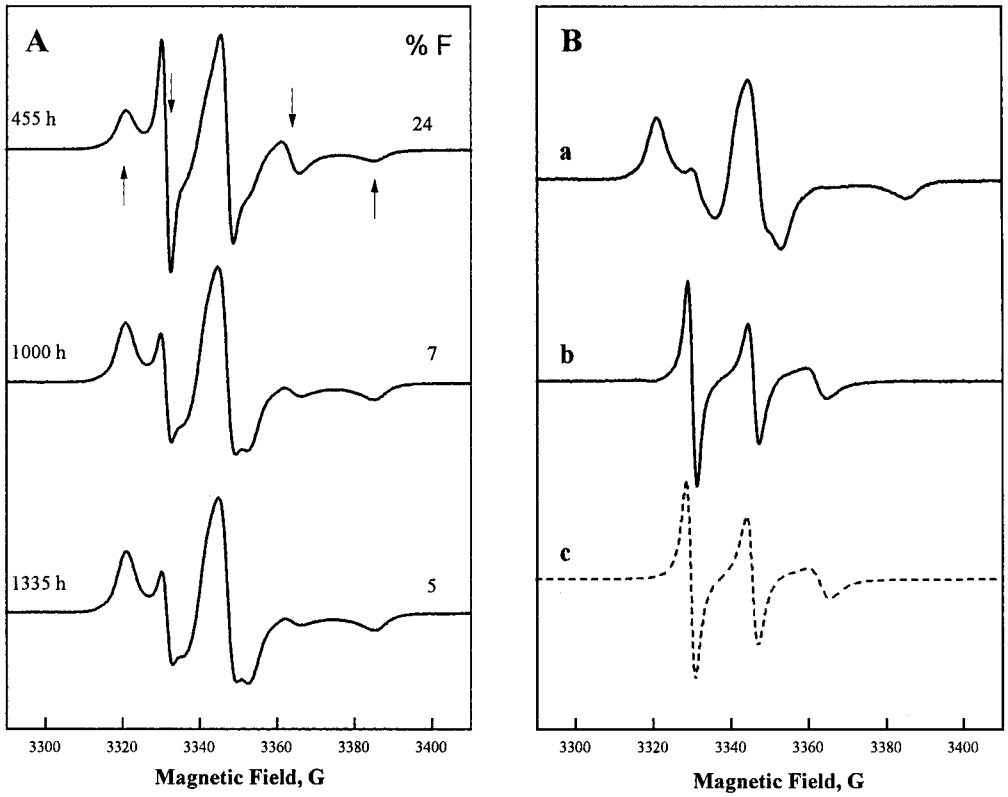

Figure 1. (A) X-band ESR spectra at 300 K of an ABS polymer containing HAS after UV irradiation times of 455, 1000, and 1335 h. Upward and downward arrows point respectively to the extreme features of the "slow" and "fast" spectral components in the top spectrum. The percentage of the "fast" component in each case is also indicated (see text). (B) Spectrum a: X-band ESR at 300 K of the irradiated ABS layer (thickness ≈0.8 mm) after UV irradiation time of 455 h. Spectrum b: ESR spectrum of the "fast" component obtained by deconvolution of the composite spectrum shown in Figure 1 for irradiation time of 455 h. Spectrum c: Calculated spectrum (dotted line), based on the following magnetic parameters: $g_{xx} = 2.0088$, $g_{yy} = 2.0061$, $g_{zz} = 2.0027$, $A_{xx} = 6.30$ G, $A_{yy} = 5.80$ G, $A_{zz} = 33.60$ G, $R_{\|} = 6.3 \times 10^8$ rad/s, $R_{\perp} = 2.5 \times 10^7$ rad/s; the line widths were $\Delta H_{\|} = 0.84$ G, $\Delta H_{\perp} = 1.24$ G, and the line shapes were a mixture of Gaussian and Lorentzian.

1D ESR Imaging. ESR spectroscopy can be transformed into an imaging method for samples containing unpaired electron spins, if the spectra are measured in the presence of magnetic field gradients.[14] The spatial resolution Δx is defined as the ratio of the line width ΔH (in G) to the field gradient G_x (in G/cm), $\Delta x = \Delta H/G_x$, implying that two signals separated by one line width due to the field gradient can be resolved.

The ESR imaging system in our laboratory consists of the Bruker 200D ESR spectrometer with a new (1998) EMX console and equipped with two Lewis coils and two regulated dc power supplies. The two sets of coils, each consisting of a figure-eight coil, are fixed on the poles of the spectrometer magnet and supply a maximum linear field gradient of ≈320 G/cm in the direction parallel to the external magnetic field (z axis) or ≈250 G/cm in the vertical direction (along the long axis, x, of the microwave resonator), with a control voltage of 20 V applied to each power supply. The coils are positioned so that the zero point of the gradient field coincides with the center of the microwave cavity. Additional details have been published.[14,15]

In 1D ESRI experiments the concentration profile is deduced from two spectra: one in the presence and one in the absence of the field gradient.[15−17] In the presence of a gradient G_x (G/cm) along the x axis, the ESR spectrum $I_C(H)$ is given by the convolution integral, eq 1,

$$I_C(H) = \int_{-\infty}^{\infty} f_0(H-H^*)\, p(H^*)\, \mathrm{d}H^* \qquad (1)$$

where $f_0(H)$ is the spectrum, H is the homogeneous stationary magnetic field, $H^* = xG_x$ is the local magnetic field (at x) due to the gradient G_x, and $p(H^*)$ is the distribution of the paramagnetic centers along the direction of the gradient. The spatial distribution of the spin probe $C(x)$ is encoded in the ESR spectrum via the magnetic field gradient G_x. The concentration profile was obtained by deconvolution of the line shape measured in the presence of gradients by the Fourier transform method[16,17] or by the entropy functional.[18] No correction for the sensitivity profile of the ESR cavity is needed if the sample is ≈4 mm long. We note that the convolution expressed in eq 1 is correct only if the ESR line shape *has no spatial dependence.*

Results and Discussion. In Figure 1A we present X-band ESR spectra at 300 K of ABS containing Tinuvin 770 for the indicated UV irradiation times in the weathering chamber. Each spectrum is a superposition of two components, from nitroxide radicals differing in their mobility: a "fast" component (F) responsible for the three-line spectrum with a total width of 32.2 G (downward arrows in the top spectrum) and a "slow" component (S) with a spectral width of 64.2 G (upward arrows). This result indicates the presence of the HAS-derived nitroxide radicals in two different environments, as a result of local heterogeneities; it is reasonable to assume that the fast and slow components reflect nitroxides located respectively in low-T_g domains dominated by polybutadiene sequences ($T_g \approx 200$ K) and in high-T_g domains dominated by polystyrene ($T_g \approx 370$

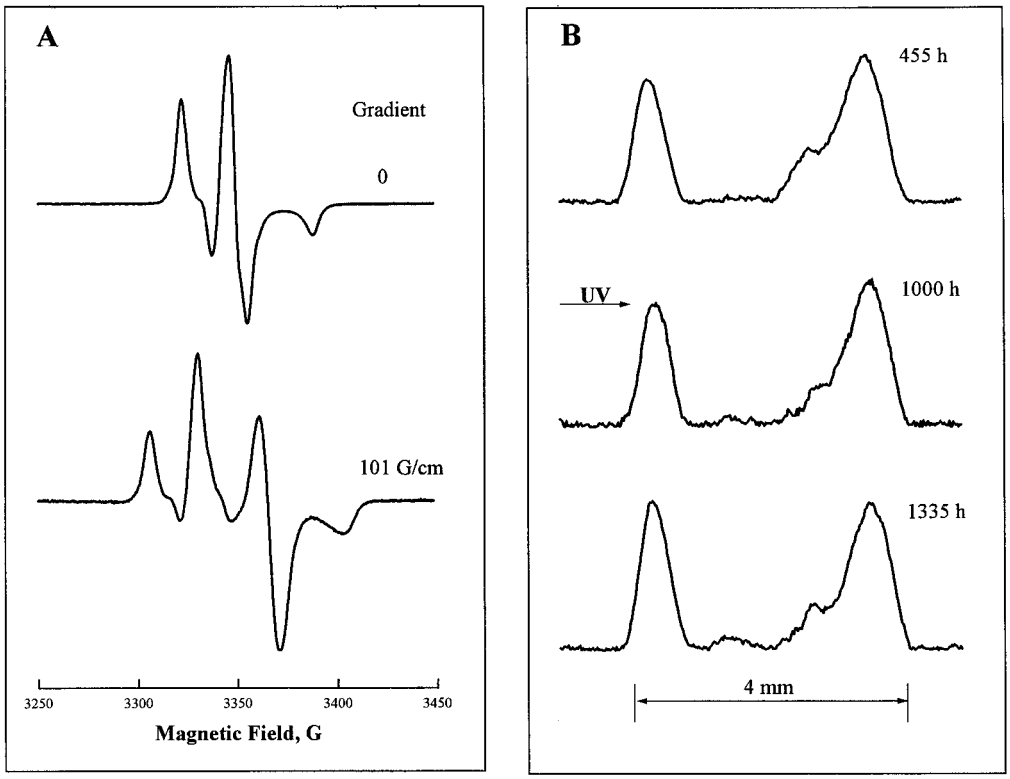

Figure 2. (A) X-band ESR spectrum at 240 K of an ABS polymer after UV irradiation in the weathering chamber for 455 h and the corresponding ESR image measured at 240 K with a magnetic field gradient of 101 G/cm. (B) Concentration profiles deduced by the Fourier method of ABS containing HAS for the indicated UV irradiation time in the weathering chamber. The horizontal arrow indicates the irradiated side of the sample.

K) or polyacrylonitrile sequences ($T_g \approx 360$ K). It is also clear from the spectra shown in Figure 1A that the relative intensity of the "fast" component decreases with increasing irradiation time. To the best of our knowledge, the presence of two spectral components for HAS-derived nitroxide radicals is reported here for the first time.

In Figure 1B we present the ESR spectrum at 300 K (spectrum a) of the directly irradiated layer of thickness ≈0.8 mm, for ABS containing HAS (irradiation time 455 h); the spectrum consists of the S component only. A similar result was obtained for the directly irradiated layers in the other samples. By subtracting the S component from the composite spectra given in Figure 1A, we deduced the line shape of the F component, as shown in Figure 1B (spectrum b). After performing a large number of such "spectral titrations", we became convinced that the line shapes of the F and S components do not vary with the irradiation time. The line widths of the three signals for the F component (spectrum b in Figure 1B) increase from low to high magnetic field. This line shape is typical of a dynamical mechanism that involves an anisotropic rotation about the N−O bond of the nitroxide[20] but can also be explained by a distribution of g and ^{14}N hyperfine tensor components.[21] We propose that the former motional mechanism is reasonable for a large molecule such as Tinuvin 770 (Chart 1). In Figure 1B we also present a simulated spectrum (dotted line, spectrum c), calculated with the magnetic parameters given in the caption and using the nonlinear-least-squares analysis method of simulation;[22] the calculated spectrum is in excellent agreement with spectrum b. In the simulation we used a $2A_{zz}$ value that is the same, within experimental error, as that measured at 120 K (68.0 ± 0.4 G) and an ^{14}N isotropic hyperfine splitting, a_N, identical to that measured at 400 K (30.5 ± 0.1 G). Spectra simulation of the F and S components (spectra a and b in Figure 1B) indicate that the corresponding rotational correlation times τ_c are $\approx 4 \times 10^{-9}$ and $\approx 5 \times 10^{-8}$ s/rad, respectively. The simulation of the S component is not shown.

On the basis of the separate spectra for the S and F components shown in Figure 1B, we reproduced all the experimental spectra shown in Figure 1A and, by double integration, deduced the ratio of the two components in the composite spectra. The percentage of the F component, % F, is 24, 7, and 5 for UV irradiation times of 455, 1000, and 1335 h, respectively. Double integration of the composite ESR spectra and comparison with a Mn^{2+}/MgO single crystal as standard indicated that the intensity of the S component is approximately constant for the above irradiation times. We propose that the decrease of the relative intensity of F with irradiation time is due to the consumption of the HAS-derived nitroxide radicals located in the butadiene-rich domains of the polymer; this scenario is plausible, as the butadiene component is expected to be more vulnerable to degradation,[23] compared to the other repeat units in ABS. The same logic can explain the absence of the F component near the irradiated side of the sample, where the high UV intensity produces more damage to the polymer.

The presence of two spectral components in the (bulk) irradiated sample, and the absence of the "fast" component near the irradiated side, suggest a spatial variation of the line shapes, which presents a problem in 1D ESRI experiments, because the convolution presented in eq 1 assumes a spatially invariant line shape. The problem was solved when we analyzed the temperature dependence of the composite spectra, such

as those shown in Figure 1A: In all composite spectra the F component appeared only at and above 260 K.[24] Below ≈260 K both spectral components, F and S, are in the slow-motional regime and have identical line shapes; the spatial variation of the line shape was thus avoided. To deduce the concentration profiles, all ESR spectra and the corresponding ESR images were therefore measured at 240 K.

In Figure 2A we present the ESR spectrum of ABS containing Tinuvin 770 and the corresponding ESR image obtained in the presence of a field gradient of 101 G/cm for an irradiation time of 455 h, both measured at 240 K. In Figure 2B we present the concentration profiles obtained by deconvolution for HAS-derived nitroxides in ABS at three UV irradiation times. The spectral resolution is ≈0.15 ± 0.05 mm (based on the broader signals at 240 K).

The larger nitroxide concentrations near the outer planes of the samples clearly indicate the role of oxygen and UV radiation in the formation of nitroxides from HAS and show the regions where the chemistry takes place. We note that the same concentration profiles were obtained when the back of the samples was covered by aluminum foil, an indication that this side is not directly irradiated. The higher nitroxide concentration at the back of the sample (not directly irradiated) can be explained by a smaller loss of nitroxide radicals due to formation of >NO•*, which transforms into diamagnetic species such as >NOH.[25]

The results presented in Figures 1 and 2 lead to several important conclusions. *First*, we demonstrated that both the concentration *and* the ESR line shapes of nitroxides in UV-irradiated ABS polymers vary along the irradiation direction. *Second*, the concentration of the HAS-derived nitroxide is low in the interior of the sample but high in a region of ≈1 mm on the irradiated sides; because oxygen and UV radiation penetrate to a depth of 50 μm at most,[26] diffusion is primarily responsible for the presence of radicals at larger depths. *Third*, the polybutadiene-rich domains in ABS polymers are most vulnerable to UV irradiation; the "fast" nitroxide component near these domains is consumed and decreases in intensity with irradiation time, and its concentration is lower where the UV irradiation is more intense. The protective mechanism of HAS appears to be specific to the system and sensitive to the morphology and thermal transitions (for instance, the glass temperature T_g) of the polymer. The results presented in this study are expected to be significant to technological application of UV and ionizing radiation: in microlithography,[27] stereolithography,[28] and curing and cross-linking of polymeric materials.[29]

Additional experiments on the time and spatial dependence of the nitroxide line shapes, on the kinetic processes responsible for the observed concentration profiles (Figure 2B), and on the degradation mechanism of HAS in the three separate homopolymers (polystyrene, polybutadiene, and polyacrylonitrile) are carried out in our laboratories.

Acknowledgment. This study was supported by the Polymers Program of the National Science Foundation and by a University Research Grant from Ford Motor Co. We thank E. J. Blais (Ford Research Laboratory) for injection molding of ABS samples, M. Lucarini (University of Bologna, Italy), and A. I. Smirnov (EPR Center, University of Illinois, Urbana) for their help with the simulation software, and J. Pilar for his participation in the initial experiments.

References and Notes

(1) Hill, D. J. T.; Le, T. T.; O'Donnell, J. H.; Perera, M. C. S.; Pomery, P. J. In *Irradiation of Polymeric Materials: Processes, Mechanisms, and Applications*, Reichmanis, E., Frank, C. W., O'Donnell, J. H., Eds.; American Chemical Society: Washington, DC, 1993.
(2) Grassie, N.; Scott, G. *Polymer Degradation and Stabilisation*; Cambridge University Press: Cambridge, U.K., 1985.
(3) O'Donnell, J. H. In *The Effects of Radiation on High-Technology Polymers*; Reichmanis, E., O'Donnell, J. H., Eds.; American Chemical Society: Washington, DC, 1989; Chapter I, p 1.
(4) Gugumus, F. In *Oxidation Inhibition in Organic Materials*; Pospisil, J., Klemchuk, P. P., Eds.; CRC Press: Boca Raton, FL, 1990; Vol. 1, p 61 and Vol. 2, p 29.
(5) Clough, R. C. In *Oxidation Inhibition in Organic Materials*; Pospisil, J., Klemchuk, P. P., Eds.; CRC Press: Boca Raton, FL, 1990; Vol. 2, p 191.
(6) Gerlock, J. L.; Bauer, D. R.; Briggs, L. M. *Polym. Degrad. Stab.* **1986**, *14*; Part I, p 53; Part II, p 73; Part III, p 97.
(7) Brede, O.; Beckert, D.; Windolph, C.; Gottinger, H. A. *J. Phys. Chem. A* **1998,** *102*, 1457. This paper provides a detailed summary of the current literature on the protective mechanism of HAS.
(8) Rabek, J. F. *Photostabilisation of Polymers, Principles and Applications*; Elsevier: London, 1990.
(9) Pospisil, J. *Adv. Polym. Sci.* **1995**, *124*, 87.
(10) *Polymer Durability: Degradation, Stabilization and Lifetime Prediction*; Clough, R. G., Billingham, N. C., Gillen K. T., Eds.; Adv. Chem. Ser. 249; American Chemical Society: Washington, DC, 1996.
(11) Denisov, E. T. *Polym. Degrad. Stab.* **1991**, *34*, *525*.
(12) *EPR Imaging and in Vivo EPR*; Eaton, G. R., Eaton, S. S., Ohno, K., Eds.; CRC Press: Boca Raton, FL, 1991.
(13) Gerlock, J. L., private communication.
(14) Schlick, S.; Pilar, J.; Kweon, S.-C.; Vacik, J.; Gao, Z.; Labsky, J. *Macromolecules* **1995**, *28*, 5780. Gao, Z.; Pilar, J.; Schlick, S. *J. Phys. Chem.* **1996**, *100*, 8430. Kruczala, K.; Gao, Z.; Schlick, S. *J. Phys. Chem.* **1996**, *100*, 11427. Gao, Z.; Schlick, S. *J. Chem. Soc., Faraday Trans.* **1996**, *92*, 4239. Malka, K.; Schlick, S. *Macromolecules* **1997**, *30*, 456. Schlick, S.; Eagle, P.; Kruczala, K.; Pilar, J. In *Spatially Resolved Magnetic Resonance: Methods, Materials, Medicine, Biology, Rheology, Ecology, Hardware*; Blümler, P., Blümich, B., Botto, R., Fukushima, E., Eds.; Wiley-VCH: Weinheim, 1998; Chapter 17, p 221. These papers describe the use of 2D spatial−spectral ESRI for measuring the diffusion coefficients of tracers.
(15) Degtyarev, E. N.; Schlick, S. *Langmuir*, in press. This study has demonstrated the application of 1D ESRI for measuring the diffusion coefficients of tracers in self-assembled polymeric surfactants.
(16) Lucarini, M.; Pedulli, G. F.; Borzatta, V.; Lelli, N. (a) *Res. Chem. Intermed.* **1996,** *22*, 581. (b) *Polym. Degrad. Stab.* **1996,** *53*, 9. (c) *Angew. Makromol. Chem.* **1997**, *252*, 179.
(17) Ahn, M. K.; Eaton, S. S.; Eaton, G. R.; Meador, M. A. B. *Macromolecules* **1997**, *30*, 8318.
(18) Smirnov, A. I.; Yakimchenko, O. E.; Golovina, H. A.; Bekova, S. K.; Lebedev, Ya. S. *J. Magn. Reson.* **1991**, *91*, 386.
(19) Allcock, H. R.; Lampe, F. W. *Contemporary Polymer Chemistry*; Prentice Hall: Englewood Cliffs, NJ, 1990; p 602.
(20) Griffith, O. H.; Jost, P. C. In *Spin Labeling: Theory and Applications*; Berliner, L. J., Ed.; Academic Press: New York, 1976; Vol. I, Chapter 12, p 453.
(21) Schlick, S.; Harvey, R. D.; Alonso-Amigo, M. G.; Klempner, D. *Macromolecules* **1989**, *22*, 822.
(22) Budil, D. E.; Lee, S.; Saxena, S.; Freed, J. H. *J. Magn. Reson. A* **1996**, *120*, 155.
(23) Carter, R. O. III; McCallum, J. B. *Polym. Degrad. Stab.* **1994**, *45*, 1.
(24) The temperature variation of the ESR spectra in the range 120−420 K indicates that the transition temperature for the "slow" component (T_{50G}) is 410 ± 3 K. The fast component appears as a three-line spectrum at ≈280 K; the splitting changes from 34.3 G at 280 K to 30.5 G at 400 K. The transition temperature for the F component occurs at a higher temperature compared to T_g of pure polybutadiene; this result can be explained by the (large) size of the probe or by the fact that the probe site is not pure polybutadiene,

but a mixture that contains the other components also. Such situations were described in our previous papers. See for example: (a) Pilar, J.; Sikora, A.; Labsky, J.; Schlick, S. *Macromolecules* **1993**, *26*, 137. (b) Muller, G.; Stadler, R.; Schlick, S. *Macromolecules* **1994**, *27*, 1555. (c) Abetz, V.; Muller, G.; Stadler, R.; Schlick, S. *Macromol. Chem. Phys.* **1995,** *196*, 3845.

(25) Keana, J. F. W.; Dinerstein, R.; Baitis, F. *J. Org. Chem.* **1971**, *36*, 209.

(26) Cao, H.; Zhang, R.; Sundar, C. S.; Yuan, J.-P.; He, Y.; Sandreczki, T. C.; Jean, Y. C.; Nielsen, B. *Macromolecules* **1998**, *31*, 6627.

(27) *The Effects of Radiation on High-Technology Polymers*; Reichmanis, E., O'Donnell, J. H., Eds.; American Chemical Society: Washington, DC, 1989.

(28) (a) Kumar, G. S.; Neckers, D. C. *Macromolecules* **1991**, *24*, 4322. (b) Fry, B. E.; Neckers, D. C. *Macromolecules* **1996**, *29*, 5306.

(29) Hoyle, C. E.; Trapp, M. A. In *Radiation Curing of Polymeric Materials*; Hoyle, C. E., Kinstle, J. E., Eds.; American Chemical Society: Washington, DC, 1990; p 429.

MA9904363